Solubilities of Phenols in Supercritical Carbon Dioxide

Philippos Coutsikos, Kostis Magoulas, and Dimitrios Tassios*

Laboratory of Thermodynamics and Transport Phenomena, Department of Chemical Engineering, National Technical University of Athens, 15780 Athens, Greece

Equilibrium solubilities of pure anthracene at 50 °C, 1-naphthol at 35, 45, and 55 °C, and hydroquinone at 35 and 45 °C in supercritical carbon dioxide over a pressure range of about 85–300 bar have been measured using a supercritical fluid extractor coupled with an external high-pressure liquid chromatographer. The solubility results, along with those for other phenols reported in the literature, are correlated with the translated-modified Peng Robinson equation of state.

Introduction

Supercritical fluids have received widespread attention during the past few years because of their potential application in extraction processes (food processing, pharmaceutical and petroleum industries, etc). The design of any particular supercritical fluid extraction process is based upon the knowledge of the solubilities of the low-volatile components in the supercritical solvents. Many researchers have shown that carbon dioxide has a high solvent potential for many organic compounds of interest, and it is one of the most important and widely used supercritical solvents for practical applications.

In this work the solubilities of the solid 1-naphthol in supercritical carbon dioxide at 35, 45, and 55 °C, as well as of solid hydroquinone (which contains two hydroxy groups) at 35 and 45 °C, are measured over a pressure range of about 85–300 bar.

Experimental Section

The solubility measurements were carried out using a sample preparation accessory (SPA) manufactured by LDC Analytical (now named Thermo Separation Products), connected with a laboratory-assembled high-perfomance liquid chromatography (HPLC), consisting on an ICI HPLC pump (model LC 1110), a Rheodyne injection valve, an APEX octadecyl symmetry reverse phase column, and an ICI LC 1200 UV/vis detector (wavelength range, 190–600 nm, wavelength accuracy, ±2 nm, and wavelength reproducibility, ±0.2 nm). Peak integration was performed with JCL 6000 Chromatography Data System software. A schematic diagram of the SPA experimental system is shown in Figure 1.

Sample Preparation Accessory (SPA). Carbon dioxide (99.995% mass purity) from the supply tank is drawn into the SPA system at ambient temperature and passes through a heat exchanger which reduces its temperature to −15 °C. It then enters the pump head which has a heat exchanger, which cools the entire pump head to approximately −10 °C. Both heat exchangers are operated by a recirculating chiller using a 50% water and 50% ethylene glycol solution as a coolant. The carbon dioxide is kept chilled through this stage to keep it in its liquid state. The carbon dioxide leaves the pump head pressurized up to 5000 psia and then it passes through a preheater where the temperature is raised above the critical temperature of CO_2 (31 °C), causing the carbon dioxide to become a supercritical fluid. It then enters the oven, where its temperature is stabilized and precisely controlled. Precise pressure control is provided by the constant pressure pump. A Sauvageau pressure gauge is connected to the outlet of the fluid pump, so that the digital pressure indication from the SPA (referred to the fluid pump outlet) can be converted in actual pressure units (bars). The oven houses the extraction loop which is made up of the six-port injector valve, the fluid cell, the recirculation pump, and the extractor. The recirculation pump operates in a constant flow mode and maintains the fluid flow within the extraction loop. In Figure 2, the SPA extraction loop is presented.

Extraction Procedure. Sample material containing the solute of interest is placed into a 5 mL 316 stainless steel extraction cup with porous bottom and top lid. The cup is then placed into the extraction loop. When the SPA system is charging, the solvent (CO_2) flows from the loop control valve through the recirculation pump and six-port injection valve and into the extractor, which has been loaded with the solute. After leaving the extractor, the CO_2 stream is passed through a high-pressure cell of a variable-wavelength UV detector. Once the desired pressure level in the loop has been reached, the extraction loop is isolated from the CO_2 supply tank and the controlled constant-pressure pump by turning the loop control valve, and then the recirculation pump is activated and the fluid is allowed to flow through the closed loop. The progress of the extraction process is monitored by the SPA UV detector, since the absorbance reading is analogous to the amount of the solute in the supercritical fluid phase. When that absorbance reading becomes constant with time, the equilibrium between the solid phase and the supercritical fluid phase has been reached.

Analysis through the HPLC System. The injection of the sample extract into the HPLC column is accomplished using the six-port injection valve and an eight-port one connected in tandem. The injection of the sample extract into the HPLC column and its passage through the HPLC detector provides a chromatogram (i.e, an absorbance vs time curve), with a peak analogous to the mass of the solute contained in the sample extract. Peak integration is performed using the appropriate software, and the obtained area value has to be converted into mass units of the solute. For that purpose, a reference curve is established for the solid of interest, that is, a relationship between the mass of the solute (injected into the column) and the area of the corresponding peak. A Rheodyne syringe loading sample injector (with a loop of 20 μL) is attached to our HPLC system in order to perform external injections

* Author to whom correspondence should be addressed.

0021-9568/95/1740-0953$09.00/0

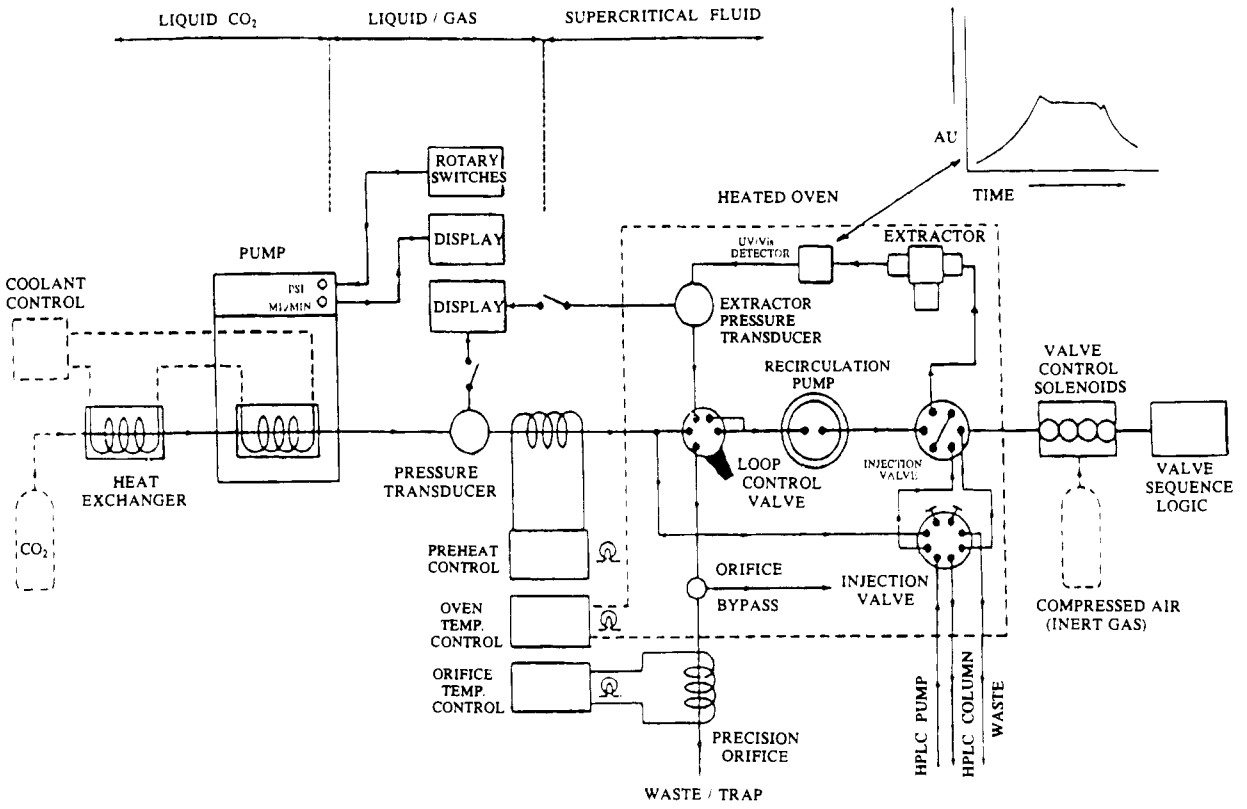

Figure 1. Schematic diagram of the sample preparation accessory apparatus.

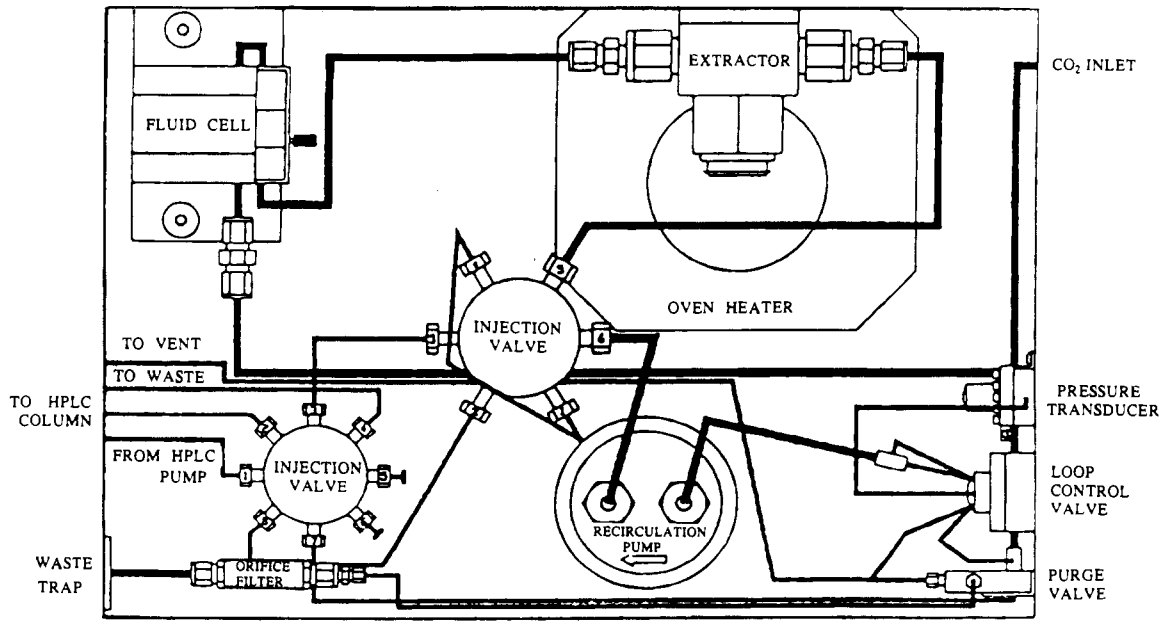

Figure 2. Extraction loop flow diagram.

from standard solutions of known concentration. Using that option of the HPLC system, the reference curve for any solute of interest can be established, provided that it absorbs significantly in the UV/vis region of the spectrum.

Hence, once the supercritical fluid (into the SPA loop) is saturated, the sample extract—which is trapped inside a 10 μL sample loop—is injected into the HPLC column and passes through the HPLC detector, providing a chromatogram peak which is converted into mass units of the dissolved solid in the sample extract through the reference curve. Since the amount of the solid solute (m) dissolved in the supercritical fluid phase has been found (for a known volume V_{SL} equal to 10 μL), the corresponding solubility (mole fraction, y_2) at the specified conditions (temperature and pressure) of the experiment is calculated from the simple following relationship:

$$y_2 = \frac{m/MW}{V_{SL}/V_{CO_2}} \quad (1)$$

under the assumption that the mixture molar volume equals approximately to the molar volume of the pure solvent (V_{CO_2}) at the same temperature and pressure. MW is the molecular weight of the solid. The pure CO_2 density is calculated through the Bender EOS (1971) with the parameters reported by Luckas and Lucas (1989).

The above assumption that the mixture molar volume equals approximately the CO_2 molar volume is expected

Table 1. Sources, Purities, and Melting Points, T_m, of the Substances Used in This Work

substance	source	purity, mass %	T_m/K
carbon dioxide	Linde	99.995	
anthracene	Merck	>96	486–489
1-naphthol	Merck	99	368–370
hydroquinone	Merck	>99	444–446

Table 2. Solubility Data, y_2, of Anthracene in Carbon Dioxide at 50 °C

P/bar	$10^5 y_2$	P/bar	$10^5 y_2$
92.6	0.310	176.5	9.881
103.0	0.327	199.4	10.900
124.8	3.247	206.1	11.036
133.4	4.665	239.6	12.543
140.3	5.502	256.3	13.362
143.3	5.449	264.4	13.516
161.2	8.124	292.6	14.671
173.5	9.256		

to be accurate for such low mole fractions of the solute in the supercritical phase.

The injection of the sample extract which is trapped inside the sample loop of the SPA apparatus is repeated several times at each pressure level; the average value of the peaks is recorded and the pressure is adjusted to the next set point. The equilibrium pressure reading is within ±0.3%, while the temperature indication of the oven is within ±0.1 °C.

Sources, purities, and melting points of the substances used in this work are listed in Table 1. All the chemicals were used without any further purification.

Experimental Results

Firstly, a number of experiments were conducted to assure that the system provides reliable solubility data. The anthracene + carbon dioxide mixture, for which solubility data have been reported from Johnston et al. (1982), was investigated at 50 °C. The reference curve for anthracene was established from 11 standard solutions, covering a concentration range from 3 to 280 mg/L, using the external injector of the HPLC system. The HPLC solvent used was methanol, and the wavelength of the HPLC detector was set equal to 254 nm. For each standard solution the injections are repeated five or six times, in order to assure the reproducibility of the obtained peaks. The standard deviation observed between the areas of the peaks for each standard solution was equal to about ±1%.

The solubility measurements were carried out according to the procedure described in the previous section. Solubility data of anthracene in supercritical carbon dioxide at 50 °C were collected for a pressure range from 93 up to 293 bar. At each equilibrium pressure, sample extract (10 μL of the supercritical mixture) injections to HPLC column were repeated about six times. For each equilibrium pressure, the average value of the obtained peaks (at 254 nm) was recorded and converted into mole fraction of the solid in the gas phase. The standard deviation observed between the areas of the peaks for each equilibrium pressure level was also equal to about ±1%.

The mole fraction solubility for anthracene at 50 °C are listed in Table 2. The comparison between anthracene solubility from this work and those reported in the literature (Johnston et al, 1982), presented in Figure 3, is very satisfactory.

Solubilities of pure 1-naphthol in supercritical carbon dioxide at three temperatures were determined. The reference curve for the 1-naphthol was established from 11 standard solutions covering a concentration range from

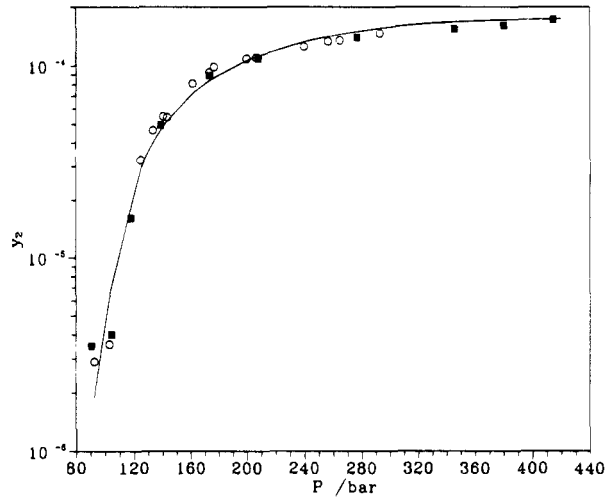

Figure 3. Solubility of anthracene in carbon dioxide at 50 °C: (○) this work, (■) Johnston et al., (—) calculated with t-mPR EOS.

Table 3. Solubility Data, y_2, of 1-Naphthol in Carbon Dioxide at 35, 45, and 55 °C

t/°C	P/bar	$10^4 y_2$	P/bar	$10^4 y_2$	P/bar	$10^4 y_2$
35	84.7	0.991	109.7	3.442	232.8	8.876
	88.2	1.449	122.2	4.698	254.2	9.117
	91.3	1.866	140.4	5.785	277.6	9.734
	96.1	2.713	163.4	6.829	293.6	10.634
	103.5	3.238	203.1	8.090		
45	88.7	0.657	109.2	4.013	173.0	10.594
	89.7	0.710	114.4	4.859	205.0	11.825
	91.5	0.742	118.5	5.469	212.3	12.437
	94.8	0.822	130.3	6.867	227.0	13.067
	96.9	1.479	144.7	8.260	262.2	13.913
	103.0	2.982	159.5	9.482	287.4	14.456
	106.6	3.519				
55	82.8	0.397	105.4	2.837	183.1	13.644
	85.6	0.448	108.2	3.284	205.0	15.418
	89.3	0.592	118.5	5.883	234.0	15.908
	91.7	0.709	127.1	8.043	251.3	16.473
	95.4	1.034	140.2	9.865	274.2	17.487
	98.5	1.184	152.4	11.682	296.5	17.875
	101.3	1.978	167.3	12.840		

35 mg/L to 1.6 g/L. The HPLC solvent used was methanol, while the chromatograms were collected at 254 nm.

The solubilities of 1-naphthol, y_2, in supercritical carbon dioxide were determined at 35, 45, and 55 °C and are given in Table 3 and in Figure 4. The accuracy of the results is estimated to be about ±25% for $y \approx 10^{-5}$ and about ±15% for $y \approx 10^{-4}$–10^{-3}, which is in agreement with those reported in the literature for these levels (Johnston et al., 1982).

Solubility data for the isomer 2-naphthol in supercritical CO_2 have been reported in the literature (Schmitt and Reid, 1986; Dobbs et al., 1987). The comparison of the solubilities of the two isomers 1-naphthol and 2-naphthol at 35, 45, and 55 °C was found to be consistent with the observation reported in the literature that the lower the melting point of an isomer, the higher the solubility in supercritical solvents at the same temperature.

Finally, solubility measurements of pure hydroquinone in supercritical CO_2 at two temperatures (35 and 45 °C) were carried out, at pressures ranging from 85 to 312 bar. The reference curve for hydroquinone was established from six standard solutions covering a concentration range from 5.5 to 35 mg/L. The HPLC solvent used was methanol, and the wavelength of the HPLC detector was set to 287 nm.

The solubilities of pure hydroquinone at 35 and 45 °C are given in Table 4 and shown in Figure 5. The solubili-

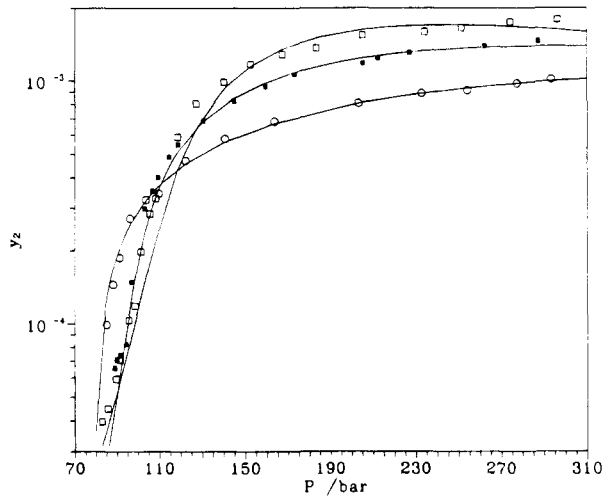

Figure 4. Solubility of 1-naphthol in carbon dioxide at different temperatures: (○) 35 °C, (■) 45 °C, (□) 55 °C, (—) calculated with t-mPR EOS.

Table 4. Solubility Data, y_2, of Hydroquinone in Carbon Dioxide at 35 and 45 °C

t/°C	P/bar	$10^5\,y_2$	P/bar	$10^5\,y_2$
35	83.6	0.336	172.7	0.881
	89.2	0.481	203.4	0.978
	92.7	0.469	229.6	1.021
	97.4	0.572	255.0	1.074
	106.1	0.591	271.8	1.139
	109.1	0.681	298.2	1.116
	135.2	0.778	311.6	1.142
	158.3	0.842		
45	85.7	0.204	168.8	1.243
	91.6	0.287	192.4	1.341
	96.2	0.428	209.7	1.358
	99.8	0.575	231.2	1.394
	108.6	0.779	249.4	1.429
	119.4	0.905	253.1	1.432
	129.5	1.065	286.3	1.470
	141.4	1.156	313.3	1.495

ties of hydroquinone (aromatic carbon ring with two hydroxy groups) are lower than those of phenol (aromatic carbon ring with one hydroxy group) by about 3 orders of magnitude. This difference is mainly due to the much lower vapor pressure of hydroquinone (0.0102 Pa at 35 °C), caused by the two hydroxy groups, as compared to that of phenol (124.46 Pa at 36 °C).

Thermodynamic Modeling

The solubilities of solids in supercritical fluids are given by eq 2

$$y_2 = \frac{P_2^{\,\mathrm{sat}} \exp[V_2^{\,S}(P - P_2^{\,\mathrm{sat}})/RT]}{\varphi_2^{\,\mathrm{SCF}} P} \qquad (2)$$

under the reasonable assumptions that no solvent dissolves in the solid phase and the solid solute is incompressible. Subscript 2 refers to the solid solute, and y_2 is the mole fraction of the solute in the fluid phase. Thus, if the solid-phase properties (molar volume, V_2^{S}, and solid vapor pressure, P_2^{sat}) are known, then the solubility of the solute in the supercritical solvent at any temperature, T, and pressure, P, can be calculated provided that an equation of state is available for the calculation of the fugacity coefficient, φ_2^{SCF}, of the solute in the supercritical fluid phase.

Correlation of the Solubility Data of Solid Phenols in CO_2. Experimental data obtained in this work along with those found in the literature were correlated with the translated and modified Peng–Robinson (t-mPR) cubic equation of state (Magoulas and Tassios, 1990). The conventional van der Waals one-fluid mixing rules are employed for the cohesion and covolume EOS parameters along with the following combining rules:

$$a_{ij} = \sqrt{(a_{ii}a_{jj})}(1 - k_{ij}) \quad \text{and} \quad b_{ij} = {}^1/_2(b_{ii} + b_{jj})(1 - l_{ij}) \qquad (3)$$

where k_{ij} and l_{ij} are binary interaction coefficients which account for the solute–solvent energetic interactions and size and shape differences, respectively. The solid solutes involved in this study are presented in Table 5, along with

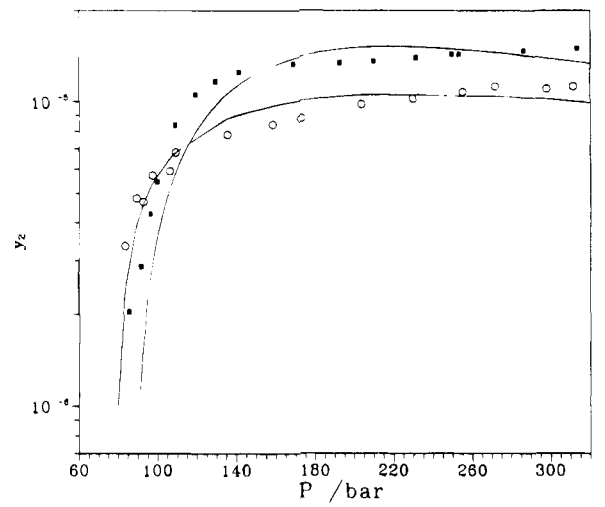

Figure 5. Solubility of hydroquinone in carbon dioxide at different temperatures: (○) 35 °C, (■) 45 °C, (—) calculated with t-mPR EOS.

Table 5. Critical Properties (T_c, P_c) and Acentric Factors (ω) for the Compounds Considered in This Work

compound	T_c/K	P_c/bar	ω	ref
anthracene	869.3	34.40	0.5320	*a*
phenol	694.3	61.30	0.4259	*b*
3,4-xylenol	729.8	48.95	0.5760	*c*
2,5-xylenol	706.9	48.00	0.5690	*d*
1-naphthol	802.0	47.37	0.5818	*e*
2-naphthol	811.4	47.37	0.5818	*e*
hydroquinone	825.2	75.61	0.6871	*e*

[a] Sheng et al. (1992). [b] Daubert and Danner (1989). [c] Mori et al. (1992). [d] Iwai et al. (1990). [e] T_c and P_c were estimated by using the Joback–Reid method; ω estimated by using the Lee–Kesler method.

Table 6. Solid Vapor Pressures and Molar Volumes for the Compounds Considered in This Study

compound	t/°C	P^{sat}/Pa	ref	V^{S}/cm^{3}mol^{-1}	ref
anthracene	50	0.02048	*a*	139.0	*b*
phenol	36	124.46	*b*	83.14	*b*
2,5-xylenol	35	12.15	*c*	125.70	*c*
3,4-xylenol	35	5.686	*c*	124.30	*c*
1-naphthol	35	0.2427	*b*	117.78	*b*
	45	0.71683	*b*		
	55	1.8872	*b*		
2-naphthol	35	0.06856	*d*	118.46	*b*
	45	0.21794	*d*		
	55	0.64561	*d*		
	70	2.92335	*d*		
hydroquinone	35	0.0102	*e*	82.67	*b*
	45	0.03528	*f*		

[a] Sheng et al. (1992). [b] Weast and Astle (1982). [c] Mori et al. (1992). [d] Schmitt and Reid (1986). [e] Lemert and Johnston (1992). [f] Estimated value.

Table 7. Correlation of Solubility of Solids (2) in Supercritical Carbon Dioxide (1) with the t-mPR Equation of State

compound	t/°C	P/bar	NDP	ref	k_{12}[a]	l_{12}[a]	%Δy_2	%Δy_2
anthracene	50	93–293	15	b	0.0967	−0.0631	12.3	
phenol	36	79–249	25	c	−0.0742	−0.3956	6.0	
2,5-xylenol	35	74–267	8	d	−0.0776	−0.4034	7.3	
3,4-xylenol	35	82–262	7	e	−0.0646	−0.3802	6.3	
2-naphthol	35	100–350	9	f	−0.0297	−0.3074	6.7	22.4
	35	103–362	6	g	0.0154	−0.2048	19.7	27.5
	35	100–362	15	f, g	−0.0083	−0.2581	14.6	
	45	103–362	6	g	−0.0414	−0.3466	6.2	12.1
	55	105–364	7	g	−0.0400	−0.3291	14.7	18.3
	70	105–364	7	g	−0.0579	−0.3778	13.2	14.3
	overall						12.0	18.9
	35–70[h]	100–362	35	f, g	−0.0334	−0.3189	15.2	
1-naphthol	35	85–294	14	b	0.0532	−0.1849	5.4	6.2
	45	89–287	19	b	−0.0431	−0.4085	9.7	10.2
	55	83–297	20	b	−0.1486	−0.6742	15.6	15.7
	overall						10.2	10.7
	35–55[h]	83–297	53	b	−0.0602	−0.4539	27.6	
all data (with one OH)					0.0134	−0.2370	33.7	
hydroquinone	35	84–312	15	b	−0.0621	−0.6515	10.7	
	45	86–313	16	b	−0.1285	−0.8867	18.5	
	overall						14.8	
	35–45[h]	84–313	31	b	−0.1060	−0.8051	16.8	

[a] k_{12} and l_{12} from eq 4. [b] Data obtained in this work. [c] Van Leer and Paulaitis (1980). [d] Iwai et al. (1990). [e] Mori et al. (1992). [f] Dobbs et al. (1987). [g] Schmitt and Reid (1986). [h] k_{12} and l_{12} are calculated for all temperatures of each system.

Table 8. Values of the Coefficients in Eq 4

	k_{ij}		l_{ij}	
system	A_0	A_1/K^{-1}	B_0	B_1/K^{-1}
CO_2 + 1-naphthol	0.1556	−0.0101	0.06677	−0.02447
CO_2 + 2-naphthol	0.005	−0.00143	0.25631	−0.002624
CO_2 + hydroquinone	0.0043	−0.00664	−0.4163	−0.02352

their critical properties (T_c, P_c) and acentric factors. For 1-naphthol and 2-naphthol as well as for hydroquinone, the critical properties have been estimated by using the Joback–Reid group contribution method, while the acentric factors were estimated using the Lee–Kesler method. Note that, because of the estimation methods, the critical pressures and the acentic factors are identical for the two isomeric naphthols. Molar volumes and sublimation pressures of the solids considered in this study are presented in Table 6.

Detailed correlation results (for the whole data base considered) using the t-mPR EOS are presented in Table 7 along with the optimum values for the binary interaction coefficients k_{ij} and l_{ij}. These correlation results are of good quality and could be used for design purposes of extraction processes for these compounds. Correlation results with the t-mPR EOS are also presented in Figures 3–5 along with the experimental data determined in this work. Notice the case of anthracene (Figure 3), where the description of the solubility data with the t-mPR equation of state is very satisfactory up to about 420 bar, while the correlation pressure range was from 93 to 293 bar.

An attempt to correlate all the isotherms of each system with one set of parameters led to errors of 15.2% for 2-naphthol, 27.6% for 1-naphthol, and 16.8% for hydroquinone, when the average errors of these systems described with temperature-dependent parameters were 12%, 10.2%, and 14.8%, respectively. Of course, these results, shown in Table 7, are not of the same quality but they are not rejectable for preliminary calculations to other temperatures of each system. Additionally, for more accurate calculations to other temperatures, the interaction coefficients k_{ij} and l_{ij} (for CO_2 + 1-naphthol, 2-naphthol, and hydroquinone systems) have been expressed as linear functions of absolute temperature:

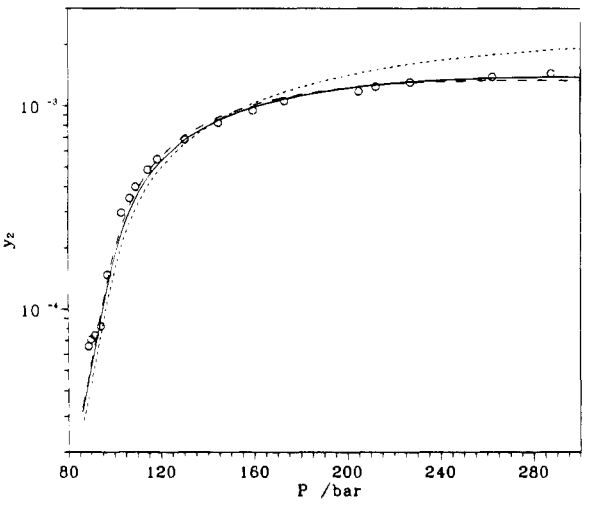

Figure 6. Description of CO_2 + 1-naphthol at 45 °C, with different sets of binary interaction parameters: (—) k_{ij} and l_{ij} system and temperature dependent, (– –) temperature independent, (- - -) system and temperature independent.

$$k_{ij} = A_0 + A_1(T - 298.15) \qquad l_{ij} = B_0 + B_1(T - 298.15) \tag{4}$$

The average results over all temperatures of each system with temperature dependent parameters are also shown in Table 7, while in Table 8 the coefficients of the k_{ij}, l_{ij} temperature functions are given.

Finally, all the available data of these aromatic alcohols with one hydroxy group were also correlated with one set of parameters. The results are also shown in Table 7, while in Figure 6 results for 1-naphthol at 45 °C are shown with three methods (k_{ij} and l_{ij} system and temperature-dependent, temperature-independent and single set for all systems). For preliminary calculations this general set can be used with an average error of 35% in solubility.

The data of hydroquinone are not included in this case since they lead to very large average errors.

Conclusions

An experimental system for providing gas–solid equilibrium data is presented in this work. The system consists

of an apparatus (SPA) for the preparation of the sample extract and an HPLC system (column, pump and UV/Vis detector) for the quantitative analysis of the sample extract. Solubility measurements of anthracene in supercritical CO_2 were carried out and were found to be in good agreement with those reported in the literature. Furthermore, experimental solubility data for pure 1-naphthol and hydroquinone are provided in order to enrich the solubility database for the CO_2–phenols systems.

The experimental data are correlated with the t-mPR EOS using two adjustable parameters (k_{ij} and l_{ij}). The results are very good for temperature-dependent parameters and acceptable for preliminary calculations for temperature-independent ones. A single set of parameters leading to errors of about 35% in the solubility of phenols with one hydroxy group in supercritical carbon dioxide is also obtained and can be used for prediction purposes in preliminary calculations involving such systems.

Literature Cited

Bartle, K. D.; Clifford, A. A.; Jafar, S. A.; Shilstone, G. F. Solubilities of Solids and Liquids of Low Volatility in Supercritical Carbon Dioxide. *J. Phys. Chem. Ref. Data* **1991**, *20*, 713–756.

Daubert, T. E.; Danner, R. P. *Data Compilation Tables of Properties of Pure Compounds*; AIChE/DIPPR, 1989.

Dobbs, J. M.; Wong, J. M.; Lahiere, R. J.; Johnston, K. P. Modification of Supercritical Fluid Phase Behavior Using Polar Cosolvents. *Ind. Eng. Chem. Res.* **1987**, *26*, 56–65.

Iwai, Y.; Yamamoto, H.; Tanaka, Y.; Arai, Y. Solubilities of 2,5- and 2,6-Xylenols in Supercritical Carbon Dioxide. *J. Chem. Eng. Data* **1990**, *35*, 174–176.

Joback, K. G.; Reid, R. C. Estimation of Pure-Component Properties from Group-Contributions. *Chem. Eng. Comm.* **1987**, *57*, 233–243.

Johnston, K.; Ziger, D.; Eckert, A. Solubilities of Hydrocarbon Solids in Supercritical Fluids. The Augmented van der Waals Treatment. *Ind. Eng. Chem. Fundam.* **1982**, *21*, 191–197.

Krukonis, V. J.; Kurnik, R. T. Solubility of Solid Aromatic Isomers in Carbon Dioxide. *J. Chem. Eng. Data* **1985**, *30*, 247–249.

Lemert, R. M.; Johnston, K. P. Chemical Complexing Agents for Enhanced Solubilities in Supercritical Fluid Carbon Dioxide. *Ind. Eng. Chem. Res.* **1991**, *30*, 1222–1231.

Luckas, M.; Lucas, R. Thermodynamic Properties of Fluid Carbon Dioxide From the SSR-MPA Potential. *Fluid Phase Equilibria* **1989**, *45*, 7–23.

Magoulas, K.; Tassios, D. Thermophysical Properties of n-Alkanes from C_1 to C_{20} and Their Prediction for Higher Ones. *Fluid Phase Equilibria* **1990**, *56*, 119–140.

Mori, Y.; Shimizu, T.; Iwai, Y.; Arai, Y. Solubilities of 3,4-Xylenol and Naphthalene + 2,5-Xylenol in Supercritical Carbon Dioxide at 35 °C. *J. Chem. Eng. Data* **1992**, *37*, 317–319.

Schmitt, W. J.; Reid, R. C. Solubility of Monofunctional Organic Solids in Chemically Diverse Supercritical Fluids. *J. Chem. Eng. Data* **1986**, *31*, 204–212.

Sheng, Y.-J.; Chen, P.-C.; Chen, Y.-P.; Wong, D. S. H. Calculations of Solubilities of Aromatic Compounds in Supercritical Carbon Dioxide. *Ind. Eng. Chem. Res.* **1992**, *31*, 967–973.

Tan, C.-S.; Weng, J.-Y. Solubility measurements of Naphthol Isomers in supercritical CO_2 by a recycle technique. *Fluid Phase Equilibria* **1987**, *34*, 37–47.

Van Leer, R. A.; Paulaitis, M. E. Solubilities of Phenol and Chlorinated Phenols in Supercritical Carbon Dioxide. *J. Chem. Eng. Data* **1980**, *25*, 257–259.

Weast, R. C.; Astle, M. J. *CRC Handbook of Chemistry and Physics*; CRC Press: Boca Raton, FL, 1982.

Received for review January 23, 1995. Accepted April 25, 1995.[⊗] The authors wish to thank European Union (EU) for the financial support in the framework of the SCIENCE program SC1-0336-C.

JE950022E

[⊗] Abstract published in *Advance ACS Abstracts,* June 1, 1995.